

pH-sensitive hydroxyethyl starch-doxorubicin conjugates as antitumor prodrugs with enhanced anticancer efficacy

Yu Zhu, Xuemei Yao, Xiaofei Chen, Li Chen

Department of Chemistry, Northeast Normal University, Changchun 130024, People's Republic of China

Correspondence to: L. Chen (E-mail: chenl686@nenu.edu.cn)

ABSTRACT: Doxorubicin (DOX) is a widely used chemotherapeutic drug for the treatment of several types of cancers, which has limitation in clinical applications because of severe heart toxicity. Herein, to reduce the fast clearance from the blood system and the severe systemic toxicity caused by the nonspecific protein adsorption, a pH-sensitive drug delivery system with higher drug conjugated content was prepared by conjugating DOX onto hydroxyethyl starch (HES) with a pH-sensitive hydrazone bond. In normal physiological environment, the release of DOX conjugated onto HES was slight which could be neglected without any side effect. However, in an acidic environment mimicking the tumor microenvironment, this pH-sensitive hydrazone linkage provided a controlled and sustained release of DOX over a period of more than 3 days. The conjugates had good biocompatibility, long circulation, and lower cytotoxicity, which could efficiently be transferred into HeLa and HepG2 cells and release the conjugated drug. Based on these promising properties, these HES-DOX conjugates outline the significant potential for future biomedical application in the controlled release of antitumor drugs. © 2015 Wiley Periodicals, Inc. *J. Appl. Polym. Sci.* **2015**, *132*, 42778.

KEYWORDS: biomaterials; drug delivery systems; stimuli-sensitive polymers

Received 26 February 2015; accepted 25 July 2015

DOI: 10.1002/app.42778

INTRODUCTION

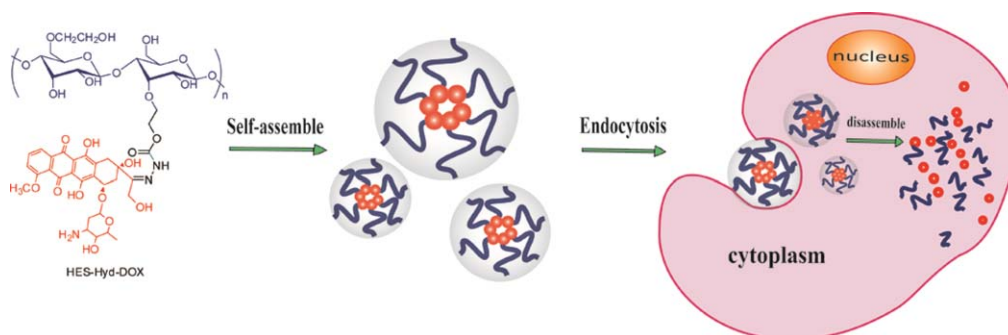
Over the past several decades, doxorubicin (DOX, Trade name: Adriamycin), as a kind of antitumor drugs, is widely used as a chemotherapeutic drug for the treatment of several types of cancers, such as lymphomas, breast, uterine, ovarian, and lung cancers.^{1,2} DOX intercalates into DNA duplex preventing DNA replication and transcription.³ However, the severe heart toxicity and serious side effects caused by nonspecific biodistribution in the body have limited the clinical application of DOX.⁴ To minus these limitations and widen the therapeutic potential of DOX, various approaches have been developed, such as chemical modification^{5–11} and loading the drugs into nanocarriers including polymeric micelles,^{12–15} vesicles,^{16,17} liposomes,^{18,19} and nanogels.^{20–22} Several nanoparticle delivery systems have been used for DOX transport *in vitro* and *in vivo*. These nanocarriers can not only increase the aqueous solubility and bioavailability of the drug but also influence pharmacokinetics and biodistribution, at the same time decrease side effects via the enhanced permeability and retention effect.^{23,24} Strategies using the unique environment of the tumor, such as pH,²⁵ temperature,²⁶ light,²⁷ redox,²⁸ and electric field²⁹ as the molecular cue to activate drug release, have received widespread attention.

Usually, there are two means to prepare delivery systems for DOX including physical encapsulation and chemical conjugation. However, DOX-loaded in nanoparticles by physical encapsulation will still unavoidably release from the encapsulated materials in physiological environment. On the other hand, the encapsulation rates of these nanoparticles are low and hardly to reach the best optimal dose because the maximum tolerated dose of DOX in humans is 60–80 mg m⁻². Compared to physical encapsulation, conjugation delivery systems have higher drug loading content, and the release of conjugated DOX in normal physiological environments can be neglected. Based on the lysosomotropism of polymer conjugates and suitable chemistry, the concept of polymer conjugate drug is developed to solve the lack of specificity of low molecular weight drugs to malignant cells. For a polymer conjugate drug, the linker between polymer and drug should be stable during transport and sensitive to disrupt at a predetermined rate in the solid tumour.^{30–32} Wang *et al.*³³ had reported the synthesis of zwitterionic polymer-based DOX conjugates, which exhibited reduced cytotoxicity, prolonged circulation time, and accelerated DOX release under mild acid conditions.

For any drug delivery to be useful practically, the most foundation consideration is its biological safety, which means good

Additional Supporting Information may be found in the online version of this article.

© 2015 Wiley Periodicals, Inc.



Scheme 1. Chemical structure of pH-sensitive HES-Hyd-DOX and intracellular microenvironment triggered release of HES-Hyd-DOX. [Color figure can be viewed in the online issue, which is available at wileyonlinelibrary.com.]

biocompatibility and biodegradability, and no toxic and no harm to normal tissues. Hydroxyethyl starch (HES), as a modified natural polysaccharide with good biocompatibility, similar to glycogen, has been used in medicine for a long time as volume therapy and is widely used colloid in a recent worldwide point prevalence study of resuscitation in intensive care units.³⁴ HES is a commonly used artificial human plasma to increase the volume of blood and maintain the blood pressure. In addition, HES has a long circulation in blood. Accordingly, in this article HES-DOX conjugates linked by pH-sensitive hydrazone bond were successfully synthesized, promising increase in the circulation time and decrease in the side effect of DOX and then increase in its antitumor efficiency (Scheme 1).

EXPERIMENTAL

Materials

HES (M_n 130 kDa, $M_w = 0.4$ Sigma), 4-nitrophenyl chloroformate (98%, Sigma), hydrazine hydrate (55%, Sigma), 3-(4,5-dimethyl-thiazol-2-yl)-2,5-diphenyl tetrazolium bromide (MTT) were purchased from Sigma-Aldrich. Doxorubicin hydrochloride (DOX-HCl) was purchased from Zhejiang Hisun Pharmaceutical. Dimethyl sulfoxide (DMSO) was dried over calcium hydride (CaH_2) and purified by vacuum distillation with CaH_2 . All the other reagents and solvents were purchased from Sinopharm Chemical Reagent and used as obtained.

Synthesis of Nitrophenyl Chloroformate-Activated HES (HES-NPC)

HES (400 mg, 0.00308 mmol) and triethylamine (TEA) (0.1 mL, 0.694 mmol) were dissolved in 10 mL of dry DMSO in a flask with N_2 protection at 25°C. 4-Nitrophenyl chloroformate (NPC) (70 mg, 0.347 mmol) was dissolved in 10 mL of dry DMSO and then dropped slowly into the flask. The mixture was stirred at 25°C for 48 h. The solution was dialyzed against deionized water for 3 days, and the product was collected by lyophilization (yield: 81%).

Conjugation of Hydrazine onto HES-NPC (HES-NHNH₂)

HES-NPC (200 mg, 0.0015 mmol) and hydrazine monohydrate (0.3 mL, 0.006 mmol) were dissolved in 10 mL of DMSO in a flask at 25°C. The mixture was stirred at 25°C for 24 h. The solution was dialyzed against deionized water for 3 days, and the product was collected by lyophilization (yield: 89%).

Conjugation of DOX onto HES (HES-Hyd-DOX)

HES-NHNH₂ (80 mg, 0.000615 mmol), DOX (108 mg, 0.186 mmol), TEA (46 μL , 0.319 mmol) were dissolved in 10 mL of dry DMSO in a flask under N_2 protection at 25°C. The mixture was stirred at 25°C for 48 h. The solution was dialyzed against DMSO for 3 days and then dialyzed against deionized water at pH 8 for 3 days. After that the product was collected by lyophilization (yield: 70%).

Conjugation of DOX onto Succinic Anhydride

Succinic anhydride (SAD) was synthesized according to the previous literature.⁹ DOX-HCl (200 mg, 0.345 mmol), SAD (41 mg, 0.414 mmol), TEA (50 μL , 0.345 mmol) were dissolved in 10 mL of dry DMSO in a flask under N_2 protection at 25°C. The mixture was stirred at 25°C for 48 h. The solution was diluted with ethyl ethanoate and then washed with saturated sodium chloride aqueous solution. The product was collected by removing ethyl ethanoate under vacuum at room temperature (yield: 68%).

Conjugation of SAD onto HES (HES-SAD)

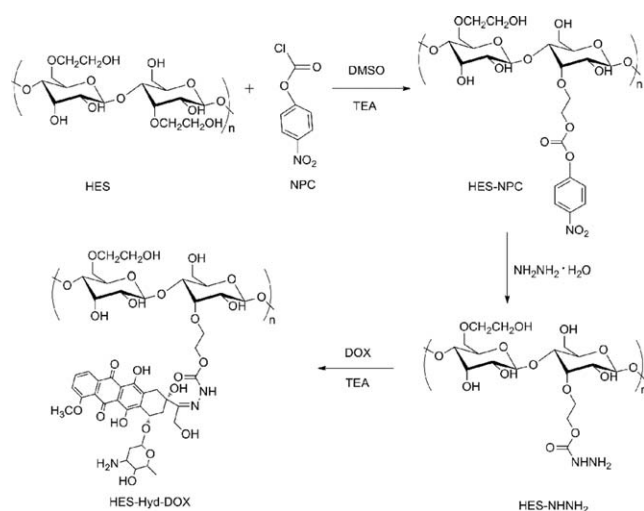
HES (70 mg, 0.00054 mmol), SAD (50 mg, 0.075 mmol), 1-ethyl-3-(3-dimethylaminopropyl) carbodiimide hydrochloride (EDC-HCl) (25 mg, 0.154 mmol), 4-dimethylaminopyridine (1.9 mg, 0.0154 mmol) were dissolved in 10 mL of DMSO in a glass ampoule with a magnetic bar. The reaction was performed at 25°C for 48 h. Then, the solvent and unreacted substances were removed by dialysis against DMSO for 72 h and then dialyzed against deionized water for 72 h. The solution was lyophilized (yield: 76%).

In Vitro Drug Conjugate and Release

To determine the drug conjugate content (DCC), the conjugates were dissolved in DMSO and analyzed by fluorescence measurement (Perkin-Elmer LS50B luminescence spectrometer) using a standard curve method ($\lambda_{\text{ex}} = 480 \text{ nm}$). The DCCs of drug-conjugated in HES-Hyd-DOX and HES-DOX were calculated according to eq. (1), respectively:

$$\text{DCC (wt \%)} = \frac{\text{amount of drug in conjugates}}{\text{amount of polymer in conjugates} \times 100} \quad (1)$$

In vitro drug release profiles of HES-Hyd-DOX (1 mg) or HES-SAD (1 mg) were investigated in phosphate buffer saline (PBS) (pH 4.0, 5.3, 6.8, or 7.4). The preweighed freeze-dried HES-Hyd-DOX 1 or HES-SAD was suspended in 4 mL of release



Scheme 2. Synthetic route for HES-Hyd-DOX conjugate.

medium and then transferred into a dialysis bag (MWCO 3500 Da). The release experiment was initiated by placing the end-sealed dialysis bag into 50 mL of release medium at 37°C with continuous shaking at 70 rpm. At predetermined intervals, 2 mL of external release medium was taken out and an equal volume of fresh release medium was replenished. The amount of released DOX was determined by using fluorescence measurement ($\lambda_{\text{ex}} = 480 \text{ nm}$). The release experiments were conducted in triplicate.

Intracellular Drug Release

The cellular uptake and intracellular release behaviors of HES-Hyd-DOX1 or HES-SAD were assessed by confocal laser scanning microscopy (CLSM) and flow cytometric analyses on HepG2 cells.

CLSM. For CLSM study, HepG2 cells were seeded in six-well plates at a density of 10^5 cells per well in complete Dulbecco's modified Eagle's medium (DMEM) containing 10% fetal bovine serum, supplemented with 50 IU mL⁻¹ penicillin and 50 IU mL⁻¹ streptomycin, and cultured for 24 h, and then incubated at 37°C for additional 2 h or 6 h with HES-Hyd-DOX 1 or HES-SAD at a final DOX concentration of 10.0 mg L⁻¹ in complete DMEM. Then, the culture medium was removed, and cells were washed with PBS thrice. Thereafter, the cells were fixed with 4% paraformaldehyde for 20 min at room temperature, and the cell nuclei were stained with 4',6-diamidino-2-phenylindole (DAPI, blue) for 5 min. CLSM images of cells were obtained through confocal microscope (Olympus FluoView 1000). The excitation wavelengths of DAPI and DOX were 405 and 488 nm, emission windows were 425–475 nm and 564–620 nm, respectively.

Flow Cytometric Analyses. HepG2 cells were seeded in six-well plates at 2×10^5 cells per well in 2.0 mL of complete DMEM, and cultured for 24 h, and then incubated at 37°C for additional 2 h with HES-Hyd-DOX 1 or HES-SAD at a final DOX concentration of 10.0 mg L⁻¹ in complete DMEM. Thereafter, the culture medium was removed, and the cells were washed with PBS thrice and treated with trypsin. Then, 2.0 mL of PBS

was added to each culture well, and the solutions were centrifuged for 5 min at 1000 rpm. After the removal of supernatants, the cells were resuspended in 0.2 mL of PBS. Data for 1×10^4 gated events were collected, and analysis was performed by flow cytometer (Beckman, CA).

Cell Viability Assays

The cytotoxicities of HES-Hyd-DOX 1 or 2 or HES-SAD against HepG2 and HeLa cells were also evaluated *in vitro* by a MTT assay. Similarly, cells were seeded into 96-well plates at 7×10^3 cells per well in 200.0 μL of complete DMEM and further incubated for 24 h. After washing cells with PBS, 180.0 μL of complete DMEM and 20.0 μL of HES-Hyd-DOXs or HES-SAD PBS solutions were added to form culture media with different DOX concentrations (0–10.0 mg L⁻¹ DOX). The cells were subjected to MTT assay after being incubated for 24, 48, and 72 h. The absorbance of the solution was measured on a Bio-Rad 680 microplate reader at 490 nm. Cell viability (%) was also calculated based on eq. (2):

$$\text{Cell viability (\%)} = A_{\text{sample}}/A_{\text{control}} \times 100 \quad (2)$$

where A_{sample} and A_{control} represent the absorbances of the sample and control wells, respectively.

RESULTS AND DISCUSSION

Preparation and Characterization of the HES-Hyd-DOX

In this work, pH-sensitive HES-Hyd-DOX prodrugs were synthesized as shown in Scheme 2. The chemical structures of HES-Hyd-DOX were confirmed by ¹H NMR, FTIR, and fluorescence measurement. There appeared the characteristic signals at 7.90, 7.63, 1.20 ppm (Figure 1) assigned to DOX indicating the successful synthesis of HES-Hyd-DOX. The absorptions at 1729 ($\nu_{\text{C=O}}$) cm⁻¹ and 1740 ($\nu_{\text{C=O}}$) cm⁻¹ (Figure 2) attributed to HES-Hyd-DOX and HES-SAD, respectively, further confirmed the chemical structure of the complex. The conjugates could assemble to form nanoparticles as listed in Table 1, this nanoscale size was suitable for entering into cells and circulation time in blood. The data of zeta potential indicated that HES-Hyd-DOX could disconnect and present positive charge at pH 4, promoting DOX to enter into cell. To determine the DCC, the conjugates were dissolved in DMSO and analyzed by fluorescence measurement using a standard curve method

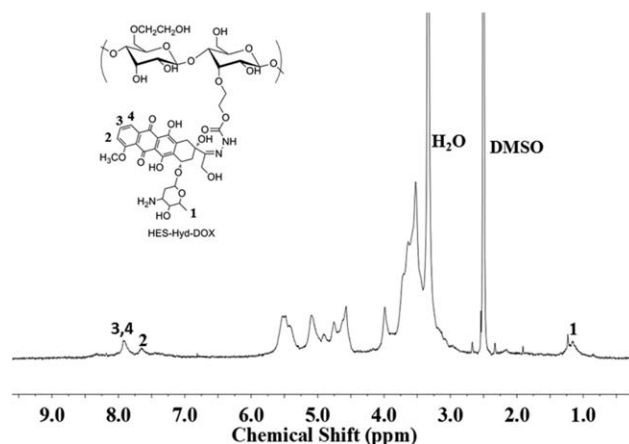


Figure 1. ¹H NMR spectrum of HES-Hyd-DOX in DMSO-*d*₆.

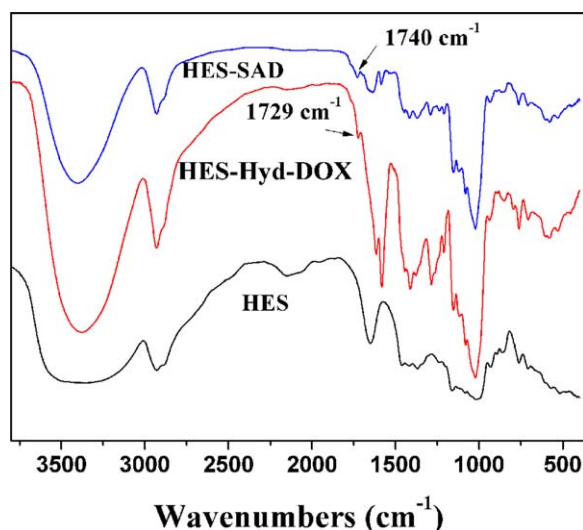


Figure 2. FTIR spectra of HES-Hyd-DOX, HES-SAD and HES. [Color figure can be viewed in the online issue, which is available at wileyonlinelibrary.com.]

($\lambda_{\text{ex}} = 480 \text{ nm}$). As expected, the DCC of HES-Hyd-DOX1, HES-Hyd-DOX12, and HES-SAD conjugates were 19%, 26%, and 9%, respectively, which had higher drug loading content than polymer micelles.¹⁴

In Vitro pH-Triggered Release

To verify the feasibility of HES-Hyd-DOX in cancer chemotherapy, a pH-insensitive HES-SAD was synthesized for comparison (Supporting Information Scheme S1 and Figure S1). The *in vitro* release behaviors were investigated at pH 4.0, 5.3, 6.8, and 7.4. The cumulative release percentages of DOX conjugated to HES by pH sensitive bond and insensitive bond versus time were plotted in Figure 3(A). Up to about 90% of DOX was released from HES-Hyd-DOX in PBS at pH 5.3 in 72 h. On the other hand, the release of DOX was much lower at pH 7.4 than 5.3. But HES-SAD exhibited not obviously different release rates at pH 4.0, 5.3, 6.8, and 7.4 [Figure 3(B)]. The different release behaviors for HES-Hyd-DOX and HES-SAD were likely resulted from the acid-triggered linker of HES and DOX. The results suggest that the HES-Hyd-DOX could effectively reduce the release of the conjugated drug in normal physiological conditions, while accelerates the drug release in response to intracellular lower pH value. These properties make the pH-sensitive HES-Hyd-DOX have tremendous potential for cancer chemotherapy.

Table I. Characterizations of Conjugates

Conjugates	DCC (wt %)	Zeta potential ^a (mV)	Zeta potential ^b (mV)	R_h^b (nm)
HES-Hyd-DOX 1	19	+8.6	0	116 ± 22
HES-Hyd-DOX 2	26	+10.3	0	94 ± 18
HES-SAD	9	0	0	153 ± 35

^a Determined at pH 4.

^b Determined at pH 7.4.

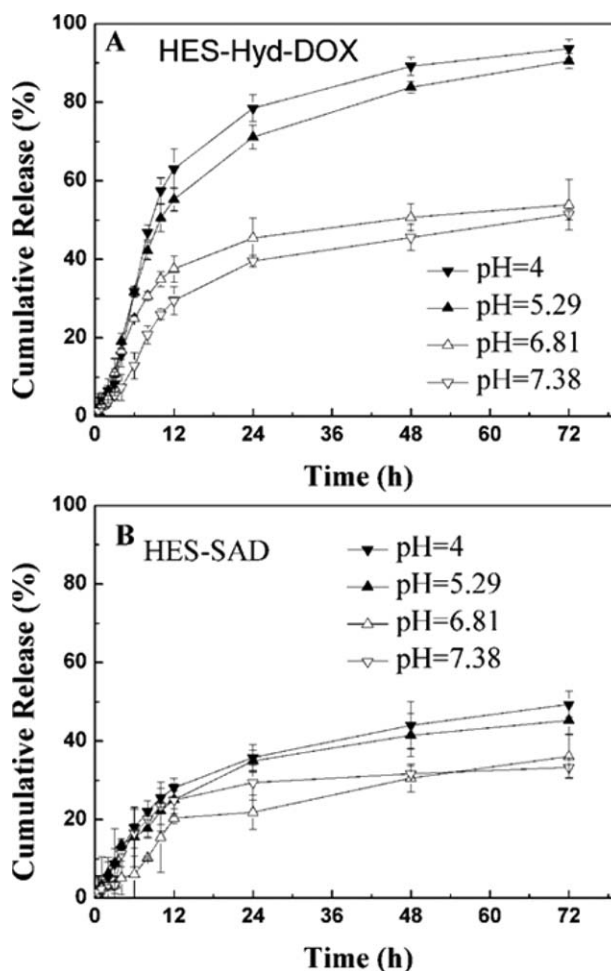


Figure 3. *In vitro* DOX release profiles for HES-Hyd-DOX1 (A) and HES-SAD (B) conjugates in PBS at 37°C at pH 4.0, 5.3, 6.8, and 7.4, respectively.

Intracellular DOX Release and Cellular Proliferation Inhibition

As a drug delivery for anticancer, the biocompatibility is very important. The *in vitro* cytotoxicity of HES against HepG2 and HeLa cells were examined by a MTT assay. Free HES did not show appreciable cytotoxicity at different concentrations, up to 10.0 g L^{-1} (Supporting Information Figures S2 and S3), indicating the excellent biocompatibility of HES itself as a drug carrier.

The cellular uptake and intracellular drug release behaviors of HES-Hyd-DOX and HES-SAD in HepG2 cells were monitored with CLSM and flow cytometry. The HES-Hyd-DOX or HES-SAD was incubated with HepG2 cells for 2 h or 6 h. As expected, stronger intracellular DOX fluorescence was detected in the cells after incubation with HES-Hyd-DOX for 6 h [Figure 4(D)] compared to those incubated with HES-SAD [Figure 4(B)]. The drug release triggered in intracellular environment was also observed by flow cytometric analyses. As shown in Figure 5(A), the flow cytometric histogram for the cells incubated with HES-Hyd-DOX shifted to the obviously higher fluorescence intensity region in contrast to that for the cells incubated

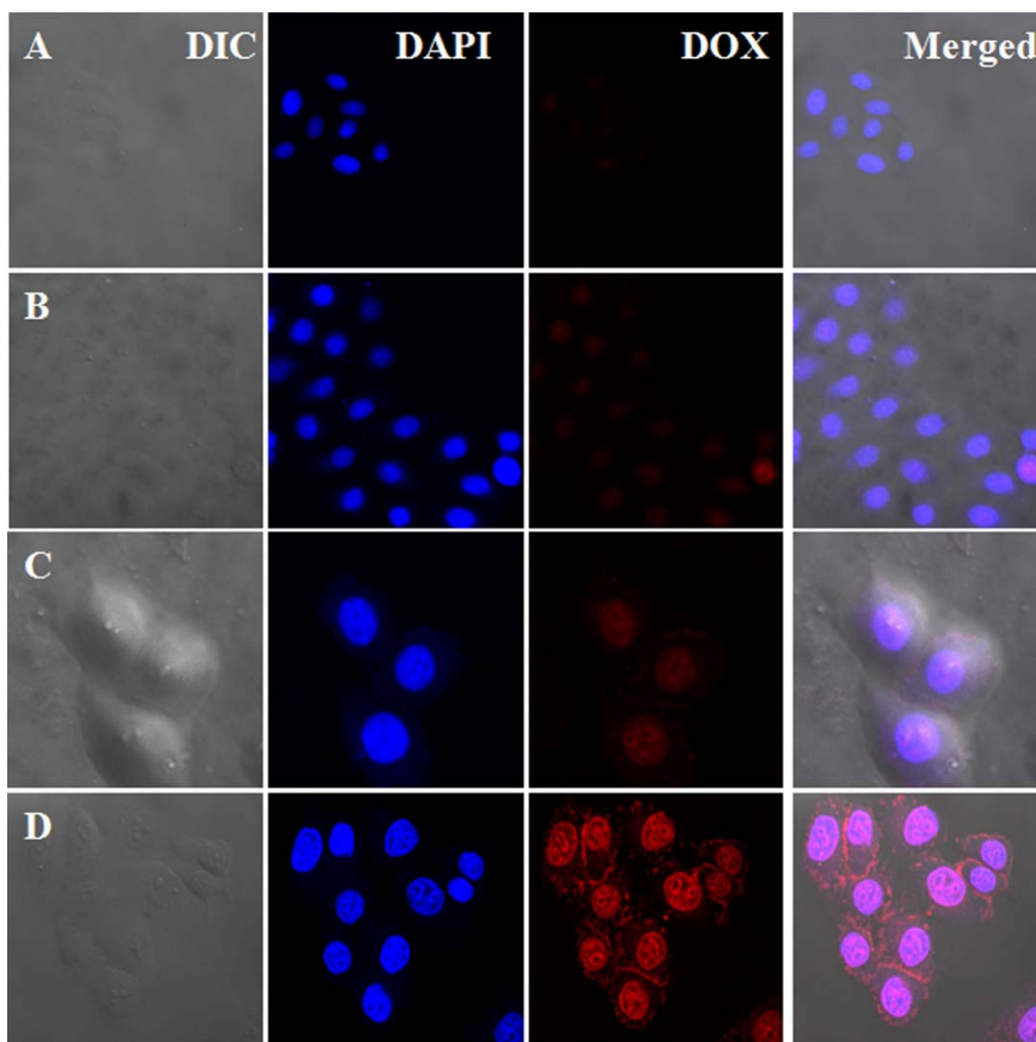


Figure 4. Representative CLSM images of HepG2 cells incubated with HES-SAD 2 h (A), HES-SAD 6 h (B), HES-Hyd-DOX 2 h (C), and HES-Hyd-DOX 6 h (D). For each panel, the images from left to right show a differential interference contrast (DIC) image, cell nuclei retained by DAPI (blue), DOX fluorescence in cells (red), and overlays of the three images. [Color figure can be viewed in the online issue, which is available at wileyonlinelibrary.com.]

with HES-SAD. The higher fluorescence intensity in the HepG2 cells incubated with HES-Hyd-DOX should result from the faster intracellular DOX release induced by acid-triggered disassociation of HES-Hyd-DOX.

At the same time, stronger intracellular drug fluorescence intensity was observed in the cells after incubation with HES-Hyd-DOX for 6 h [Figure 4(D)] than 2 h [Figure 4(C)]. In contrast, there was hardly any difference of fluorescence intensity shown

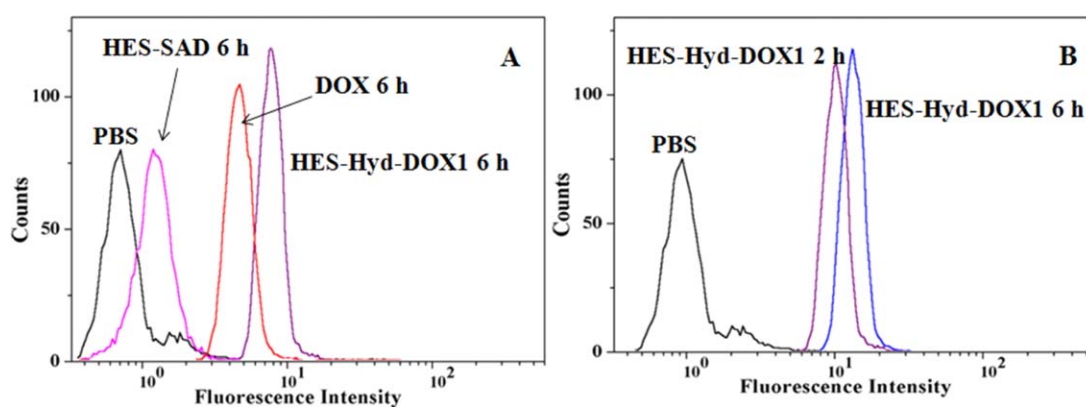


Figure 5. Flow cytometry profiles of HepG2 cells incubated with (A) PBS, HES-SAD 6 h, DOX 6 h, HES-Hyd-DOX1 6 h; (B) HES-Hyd-DOX1 for 2 h and for 6 h. [Color figure can be viewed in the online issue, which is available at wileyonlinelibrary.com.]

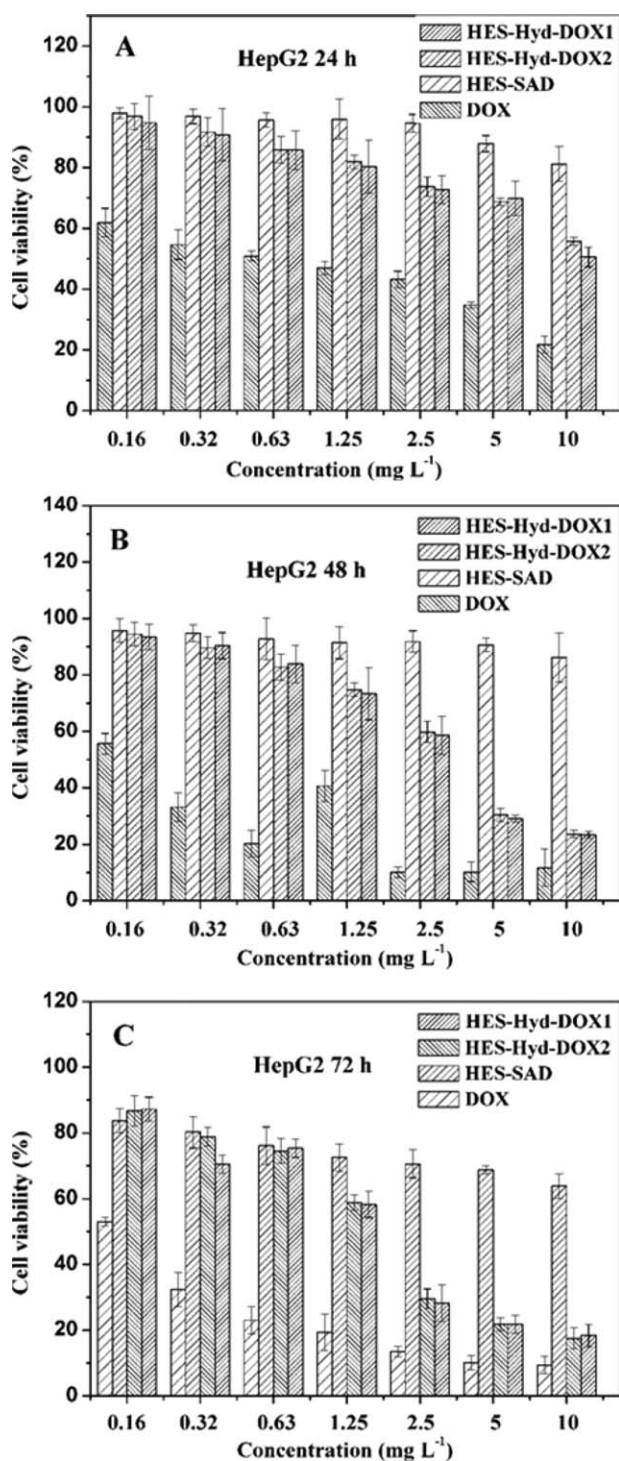


Figure 6. Cytotoxicity of HES-Hyd-DOX and HES-SAD toward HepG2 cells after incubation for 24 h (A), 48 h (B) and 72 h (C).

in the cells incubated with HES-SAD for 6 h [Figure 4(B)] and 2 h [Figure 4(A)]. Meanwhile, the flow cytometric histograms of cells incubated with HES-Hyd-DOX for 6 h also shifted clearly to the direction of high fluorescence intensity compared with 2 h as shown in Figure 5(B). The higher fluorescence intensity in the HepG2 cells incubated for 6 h with HES-Hyd-DOX should result from the intracellular DOX release induced

by acid-triggered disassociation of HES-Hyd-DOX, implying that the drug release of HES-Hyd-DOX was controlled release.

The *in vitro* cellular proliferation inhibitions of HES-Hyd-DOX and HES-SAD against HepG2 cells (Figure 6) and HeLa cells (Supporting Information Figure S2) were also estimated using a MTT assay. As shown in Figure 6, in contrast to HES-SAD, HES-Hyd-DOX exhibited significantly higher growth inhibition efficiency to HeLa cells at 24 h, 48 h, and 72 h. Moreover HES-Hyd-DOX also exhibited significantly higher growth inhibition efficiency to HeLa (Supporting Information Figure S4). The results revealed that the DOX release HES-Hyd-DOX was triggered by the endosomal pH environment, leading to enhanced inhibition of cell proliferation as compared with the pH-insensitive HES-SAD. The HES-Hyd-DOX provided an efficient drug delivery platform for inhibition of different cancer cells.

CONCLUSION

In summary, acid-insensitive HES-SAD and acid-sensitive HES-Hyd-DOX were successfully prepared. Their chemical structures were confirmed by ¹H NMR and FTIR, respectively. *In vitro* drug release from HES-Hyd-DOX could be accelerated in acidic conditions mimicking the endosomal/lysosomal compartments. HES-Hyd-DOX exhibited faster DOX release behavior in HepG2 cells than that pH-insensitive HES-SAD. Moreover, a higher cellular proliferation inhibition efficacy was achieved. HES-Hyd-DOX, which has a higher molecular weight, excellent biocompatibility, and smart intracellular microenvironment responsiveness could reduce toxicity and improve anticancer efficacy with a great potential for cancer chemotherapy.

ACKNOWLEDGMENTS

This research was financially supported by the National Natural Science Foundation of China (Projects 51273037, 50903012, 21174142), Jilin Science and Technology Bureau (International Cooperation Project 20120729, 20130206074GX), and Jilin Human Resources and Social Security Bureau (201125020).

REFERENCES

- Vincenzi, B.; Frezza, A. M.; Santini, D.; Tonini, G. *Expert Opin. Emerg. Drugs* **2010**, *15*, 237.
- Hortobagyi, G. N. *Drugs* **1997**, *54* (Suppl 4), 1.
- Swift, L. P.; Rephaeli, A.; Nudelman, A.; Phillips, D. R.; Cutts, S. M. *Cancer Res.* **2006**, *66*, 4863.
- Octavia, Y.; Tocchetti, C. G.; Gabrielson, K. L.; Janssens, S.; Crijns, H. J.; Moens, A. L. *J. Mol. Cell. Cardiol.* **2012**, *52*, 1213.
- Soudy, R.; Chen, C.; Kaur, K. *J. Med. Chem.* **2013**, *56*, 7564.
- Du, J.-Z.; Du, X.-J.; Mao, C.-Q.; Wang, J. *J. Am. Chem. Soc.* **2011**, *133*, 17560.
- Liu, P.; Shi, B.; Yue, C.; Gao, G.; Li, P.; Yi, H. *Polym. Chem.* **2013**, *4*, 5793.
- Tavano, L.; Muzzalupo, R.; Mauro, L.; Pellegrino, M.; Andò, S.; Picci, N. *Langmuir* **2013**, *29*, 12638.

9. Ding, J.; Shi, F.; Li, D.; Chen, L.; Zhuang, X.; Chen, X. *Biomater. Sci.* **2013**, *1*, 633.
10. Pan, H.; Sima, M.; Yang, J.; Kopecek, J. *J. Macromol. Biosci.* **2013**, *13*, 155.
11. Okeley, N. M.; Toki, B. E.; Zhang, X.; Jeffrey, S. C.; Burke, P. J.; Alley, S. C. *Bioconjugate Chem.* **2013**, *24*, 1650.
12. Zhang, Z.; Chen, X.; Chen, L.; Yu, S.; Cao, Y.; He, C. *ACS Appl. Mater. Interfaces* **2013**, *5*, 10760.
13. Zhang, C. Y.; Yang, Y. Q.; Huang, T. X.; Zhao, B.; Guo, X. D.; Wang, J. F. *Biomaterials* **2012**, *33*, 6273.
14. Zhang, Z.; Ding, J.; Chen, X.; Xiao, C.; He, C.; Zhuang, X. *Polym. Chem.* **2013**, *4*, 3265.
15. Zhang, Y.; Xiao, C.; Li, M.; Chen, J.; Ding, J.; He, C. *Macromol. Biosci.* **2013**, *13*, 584.
16. Yuk, S. H.; Oh, K. S.; Koo, H.; Jeon, H.; Kim, K.; Kwon, I. C. *Biomaterials* **2011**, *32*, 7924.
17. Yang, X.; Grailler, J. J.; Rowland, I. J.; Javadi, A.; Hurley, S. A.; Matson, V. Z. *ACS Nano* **2010**, *4*, 6805.
18. Du, Y.; Chen, W.; Zheng, M.; Meng, F.; Zhong, Z. *Biomaterials* **2013**, *33*, 7291.
19. Bochot, A.; Fattal, E. *J. Control Release* **2012**, *161*, 628.
20. Ding, J.; Zhuang, X.; Xiao, C.; Cheng, Y.; Zhao, L.; He, C. *J. Mater. Chem.* **2011**, *21*, 11383.
21. Chacko, R. T.; Ventura, J.; Zhuang, J.; Thayumanavan, S. *Adv. Drug Deliv. Rev.* **2012**, *64*, 836.
22. Oh, J. K.; Drumright, R.; Siegwart, D. J.; Matyjaszewski, K. *Progr. Polym. Sci.* **2008**, *33*, 448.
23. Lammers, T.; Kühnlein, R.; Kissel, M.; Subr, V.; Etrych, T.; Pola, R. *J. Control Release* **2005**, *110*, 103.
24. Fang, J.; Nakamura, H.; Maeda, H. *Adv. Drug Deliv. Rev.* **2011**, *63*, 136.
25. Lin, L.; Cong, Z.-X.; Li, J.; Ke, K.; Guo, S.-S.; Yang, H. *J. Mater. Chem. B* **2014**, *2*, 1031.
26. Chen, L.; Tian, Y.-K.; Ding, Y.; Tian, Y.-J.; Wang, F. *Macromolecules* **2012**, *45*, 8412.
27. Wang, C.; Chen, Q.; Xu, H.; Wang, Z.; Zhang, X. *Adv. Mater.* **2010**, *22*, 2553.
28. Shi, F.; Ding, J.; Xiao, C.; Zhuang, X.; He, C.; Chen, L. *J. Mater. Chem.* **2012**, *22*, 14168.
29. Yan, Q.; Yuan, J.; Cai, Z.; Xin, Y.; Kang, Y.; Yin, Y. *J. Am. Chem. Soc.* **2010**, *132*, 9268.
30. Fanciullino, R.; Ciccolini, J.; Milano, G. *Crit. Rev. Oncol. Hematol.* **2013**, *88*, 504.
31. Mahmud, A.; Xiong, X. B.; Lavasanifar, A. *Eur. J. Pharm. Biopharm.* **2008**, *69*, 923.
32. Pang, X.; Yang, X.; Zhai, G. *Expert Opin. Drug Deliv.* **2014**, *11*, 1075.
33. Wang, Z. G.; Zhang, J.; Lin, W.; Ji, F.; Bernards, M. T. *Langmuir* **2014**, *30*, 3764.
34. Yang, J.; Gao, C.; Lü, S.; Zhang, X.; Yu, C.; Liu, M. *Carbohydr. Polym.* **2014**, *102*, 838.